Eur. Phys. J. D **30**, 403–410 (2004)
DOI: 10.1140/epjd/e2004-00094-2

THE EUROPEAN PHYSICAL JOURNAL D

Coherent-state qubits: entanglement and decoherence

J.K. Asbóth[1,2,a], P. Adam[2,3], M. Koniorczyk[2,4], and J. Janszky[2,3]

[1] Institut für Theoretische Physik, Universität Innsbruck, Technikerstrasse 25, 6020 Innsbruck, Austria
[2] Research Institute for Solid State Physics and Optics, P.O. Box 49, 1525 Budapest, Hungary
[3] Research Group for Nonlinear and Quantum Optics, Hungarian Academy of Sciences and Institute of Physics, University of Pécs, Ifjúság út 6, 7624 Pécs, Hungary
[4] Research Centre for Quantum Information, Institute of Physics, Slovak Academy of Sciences, 845 11 Dubravská cesta 9, Bratislava, Slovakia

Received 30 January 2004 / Received in final form 13 May 2004
Published online 10 August 2004 –

Abstract. Arbitrary superpositions of any two optical coherent states are investigated as realizations of qubits for quantum information processing. Decoherence of these coherent-state qubits is described in detail, and visualized using a suitable adaptive Bloch-sphere. The entanglement that can be created by a beam splitter from these states is quantified, and its decoherence behavior is analyzed.

PACS. 42.50.Dv Nonclassical states of the electromagnetic field, including entangled photon states; quantum state engineering and measurements – 03.65.Ud Entanglement and quantum nonlocality (e.g. EPR paradox, Bell's inequalities, GHZ states, etc.) – 03.67.-a Quantum information

1 Introduction

Coherent states are the most classical of the quantum states of a radiation field. Quantum superpositions of two distinct coherent states are therefore often called "Schrödinger cats", referring to the famous gedanken experiment [1]. Typical examples are the even and odd coherent states, introduced by Dodonov et al. [2]. Schrödinger cats have been prepared in microwave cavities [3], on motional quantum states of trapped ions [4], and there are proposals for preparation of a single-mode radiation field in such states [5–8].

The superpositions of coherent states have interesting physical features [9]. Two coherent states are never orthogonal, and their superpositions form a two-dimensional Hilbert-space. Thus given two fixed coherent sates one may represent a qubit. This opens the possibility of using coherent states for quantum information processing (QIP) [10–13].

In QIP applications it is necessary for *all* superpositions of the computational basis states to be robust against decoherence. The decoherence of Schrödinger cats was extensively studied, primarily in terms of nonclassical features and phase-space distributions [14–20]. In this paper we give a full description of the decoherence properties of the coherent-state superpositions, from the special point of view of a qubit representation. We visualize the evolution of these states on a suitably defined Bloch sphere.

[a] e-mail: janos.asboth@uibk.ac.at

The most important resource of QIP is quantum entanglement. In quantum optics a possible way to create an entangled state of two modes of light field is letting a single mode interfere with another mode in vacuum state on a beam splitter. The so available entanglement is strongly related to the nonclassicality of the initial state of the field [21,22]. We examine coherent-state superpositions from this aspect. We explicitly calculate the amount of entanglement that can be created from any single-mode coherent-state superposition using a beam splitter. The entangled states generated this way are termed "two-mode Schrödinger cats" or "entangled coherent states".

Once entanglement is generated, it is very important to know how much it will be deteriorated due to environmental decoherence. The facet of the fidelity of teleportation [10] and the negativity [11] have already been subjects of studies in the specific case of an entangled coherent state with maximal entanglement. A physically informative measure is the entanglement of formation, calculated by Li and Xu [20] for a class of entangled coherent states also during their decoherence. We extend these studies to two-mode entangled states resulting from arbitrary superpositions of two coherent states. In this way we treat a wider class of two-mode states. A simple picture emerges regarding the fraction of entanglement left in the state.

This paper is organized as follows: in Section 2 we introduce coherent-state qubits and the Bloch sphere as used throughout the paper. In Section 3 our results concerning decoherence of a single coherent-state qubit are presented. Section 4 describes the creation of

entanglement from these states using a beam splitter, and how this is affected by decoherence. In Section 5 our results are summarized and the conclusions are drawn.

2 Coherent-state superpositions as qubits

Throughout this paper we examine superpositions of coherent states of single mode light fields:

$$|\Psi\rangle = c_1 |\alpha_1\rangle + c_2 |\alpha_2\rangle \tag{1}$$

where c_1 and c_2 are complex numbers, and $|\alpha_k\rangle$ denotes a coherent state. With fixed α_1 and α_2, a two dimensional Hilbert space is spanned by these superpositions, thus the system realizes a quantum bit. We rewrite the state $|\Psi\rangle$ with the Weyl displacement operator $\hat{D}$ as:

$$|\Psi\rangle = \hat{D}(\beta)\left(c_1\, e^{i\chi}\,|\alpha\rangle + c_2\, e^{-i\chi}\,|-\alpha\rangle\right), \tag{2}$$

using $\beta = (\alpha_1 + \alpha_2)/2$, $\alpha = (\alpha_1 - \alpha_2)/2$, and $\chi = \mathrm{Im}\beta\alpha^*$. The following notation is used for the overlap of the constituent coherent states $|\alpha_1\rangle$ and $|\alpha_2\rangle$:

$$\langle\alpha_1|\alpha_2\rangle = a\, e^{-2i\chi}; \quad a = \exp\left(-2\,|\alpha|^2\right). \tag{3}$$

When discussing decoherence of these states, we have to consider mixtures of coherent-state superpositions of the form (1). The states constituting the mixture have the same coherent-state amplitudes α_1 and α_2, but different probability amplitudes c_i. The density operator of such a mixture reads:

$$\begin{aligned}\hat{\varrho} &= \sum_k p_k\,|\Psi_k\rangle\langle\Psi_k| \\ &= \varrho_{00}\,|\alpha_1\rangle\langle\alpha_1| + \varrho_{01}\,|\alpha_1\rangle\langle\alpha_2| \\ &\quad + \varrho_{10}\,|\alpha_2\rangle\langle\alpha_1| + \varrho_{11}\,|\alpha_2\rangle\langle\alpha_2|, \quad \sum_k p_k = 1.\end{aligned} \tag{4}$$

The coefficients c_k in equation (1) and ϱ_{km} in equation (4) can be written in a vector and matrix form, respectively:

$$|\Psi\rangle \rightsquigarrow \mathbf{c} = \begin{pmatrix} c_1 \\ c_2 \end{pmatrix}; \quad \hat{\varrho} \rightsquigarrow \boldsymbol{\varrho} = \begin{pmatrix} \varrho_{00} & \varrho_{01} \\ \varrho_{10} & \varrho_{11} \end{pmatrix}. \tag{5}$$

Notice that the basis vectors $|\alpha_1\rangle$ and $|\alpha_2\rangle$ are not orthogonal, therefore $\mathbf{c}$ and $\boldsymbol{\varrho}$ are not a state vector and a density matrix in the usual sense. Their normalization is:

$$|c_1|^2 + |c_2|^2 + 2a\mathrm{Re}\left(c_1^* c_2 e^{-2i\chi}\right) = 1, \tag{6}$$

$$\varrho_{00} + \varrho_{11} + 2a\mathrm{Re}\left(\varrho_{10} e^{-2i\chi}\right) = 1. \tag{7}$$

If, however, $|\alpha| \gg 1$, then $a \ll 1$, and $|\alpha\rangle$ and $|-\alpha\rangle$ are almost orthogonal, therefore their use as computational basis states results in only small errors. This allows effective quantum computation as described by Jeong and Kim [12] and analyzed by Ralph et al. [13]. It is also possible to stick to the nonorthogonal coherent-state basis and take into account the nonzero overlap a by introducing a metric tensor $G_{ik} = \langle\alpha_i|\alpha_k\rangle$, as in [23]. In this article we follow a different approach, by choosing an appropriate orthogonal basis.

In the $\beta = 0$ case the symmetric and antisymmetric superpositions

$$|\pm\rangle_0 = (\mathcal{N}_\pm)^{-\frac{1}{2}}\left(|\alpha\rangle \pm |-\alpha\rangle\right) \tag{8}$$

play a special role. Here $\mathcal{N}_\pm = 2(1 \pm a)$ are normalizing factors. These were called "even" and "odd" coherent states by Dodonov et al. [2], since their Fock state decomposition consists of states with only even, or odd number of photons. It follows immediately that they are orthogonal, and thus form an orthonormal basis in the two-dimensional Hilbert space spanned by the coherent states $|\alpha\rangle$ and $|-\alpha\rangle$. Displacing these states by $\hat{D}(\beta)$ we obtain an orthogonal basis we call "qubit basis" in what follows:

$$|\pm\rangle = \hat{D}(\beta)\,|\pm\rangle_0 = (\mathcal{N}_\pm)^{-\frac{1}{2}}\left(e^{-i\chi}\,|\alpha_1\rangle \pm e^{i\chi}\,|\alpha_2\rangle\right). \tag{9}$$

On this basis, pure states are represented by vectors $\mathbf{y}$ and mixed states by matrices $\boldsymbol{\sigma}$ as usual:

$$\begin{aligned}|\Psi\rangle &= y_1\,|+\rangle + y_2\,|-\rangle\,; \\ \hat{\varrho} &= \sigma_{00}\,|+\rangle\langle+| + \sigma_{01}\,|+\rangle\langle-| \\ &\quad + \sigma_{10}\,|-\rangle\langle+| + \sigma_{11}\,|-\rangle\langle-|\,.\end{aligned} \tag{10}$$

To link the nonorthogonal coherent-state $|\pm\alpha\rangle$, and the orthogonal qubit $|\pm\rangle$ basis, we introduce the non-unitary transformation matrix $\mathbf{T}$:

$$\begin{aligned}\mathbf{T} &= \frac{1}{2}\begin{pmatrix} e^{i\chi}\,(\mathcal{N}_+)^{\frac{1}{2}} & e^{-i\chi}\,(\mathcal{N}_+)^{\frac{1}{2}} \\ e^{i\chi}\,(\mathcal{N}_-)^{\frac{1}{2}} & -e^{-i\chi}\,(\mathcal{N}_-)^{\frac{1}{2}} \end{pmatrix} \\ &\Updownarrow \\ \mathbf{T}^{-1} &= \begin{pmatrix} e^{-i\chi}\,(\mathcal{N}_+)^{-\frac{1}{2}} & e^{-i\chi}\,(\mathcal{N}_-)^{-\frac{1}{2}} \\ e^{i\chi}\,(\mathcal{N}_+)^{-\frac{1}{2}} & -e^{i\chi}\,(\mathcal{N}_-)^{-\frac{1}{2}} \end{pmatrix}.\end{aligned} \tag{11}$$

The following relations link the two representations of a given pure or mixed state:

$$\mathbf{y} = \mathbf{T}\mathbf{c}, \quad \boldsymbol{\sigma} = \mathbf{T}\boldsymbol{\varrho}\mathbf{T}^\dagger; \quad \mathbf{c} = \mathbf{T}^{-1}\mathbf{y}, \quad \boldsymbol{\varrho} = \mathbf{T}^{-1}\boldsymbol{\sigma}\mathbf{T}^{-1\dagger}, \tag{12}$$

where $\mathbf{T}^\dagger$ is the adjoint of the matrix $\mathbf{T}$. We remark that the transformation matrix $\mathbf{T}$ is the "square root" of the metric tensor, in the sense that $\mathbf{T}^\dagger\mathbf{T} = \mathbf{G}$.

2.1 Bloch sphere

The matrix $\boldsymbol{\sigma}$ introduced in (10) is the density matrix of a two-level system expanded on the orthonormal basis $|\pm\rangle$. This allows us to use the standard Bloch-sphere picture, as depicted in Figure 1. We write

$$\boldsymbol{\sigma} = \frac{1}{2}\begin{pmatrix} 1 + P_3 & P_1 - iP_2 \\ P_1 + iP_2 & 1 - P_3 \end{pmatrix} \tag{13}$$

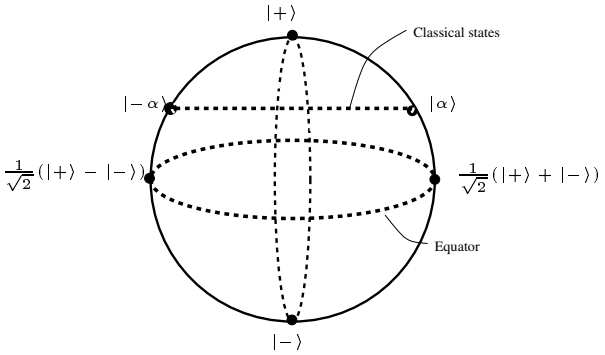

Fig. 1. The Bloch sphere of mixtures coherent-state superpositions. The classicality line is the set of points representing states that are mixtures of coherent states.

where the real numbers P_1, P_2 and P_3 are the pseudospin components. The positivity of $\boldsymbol{\sigma}$ implies $(P_1)^2 + (P_2)^2 + (P_3)^2 < 1$. Thus the pseudospin components representing the state define a point inside a unit 3-dimensional sphere, the Bloch sphere.

Pure states lie on the surface of the Bloch sphere, and can be parametrized with the polar angles θ and ϕ:

$$|\Psi\rangle = \cos\frac{\theta}{2}\,|+\rangle + e^{i\phi}\sin\frac{\theta}{2}\,|-\rangle\,. \tag{14}$$

The north pole is $|+\rangle$, the south pole $|-\rangle$. The two constituent coherent states $|\alpha\rangle$ and $|-\alpha\rangle$ lie on the surface of the Bloch sphere north of the equator, they both have polar angle $\theta = \cos^{-1}(a)$, and their azimuthal angles are $\phi = 0$ and $\phi = \pi$, respectively. The set of "classical states", i.e. statistical mixtures of coherent states lies on the line connecting the points $|\alpha\rangle$ and $|-\alpha\rangle$. We call this set, given by $P_2 = 0$ and $P_3 = a$, the classicality line. If $|\alpha| \gg 1$, then $a \ll 1$, and the classicality line goes almost through the center of the sphere, the state with highest entropy. If $|\alpha| \ll 1$, then $a \approx 1$, and the classicality line is practically at the North pole. This is easily understood, since in the limit as $\alpha \to 0$, the even and odd coherent states tend to the $|0\rangle$ and $|1\rangle$ Fock states, respectively.

It should be noted that the Bloch sphere is introduced for a fixed coherent amplitude. For a decohering state, the decrease of the coherent amplitude will change the notion of the Bloch sphere itself. This leads naturally to the adaptive Bloch sphere, discussed in Section 3.

3 Decoherence of a coherent-state qubit on the adaptive Bloch sphere

In quantum optics a lossy transmission line, e.g. an optical fiber is usually modeled by a series of beam splitters. This simple model is an appropriate description for most practical situations. Throughout this paper we use the standard description of the beam splitters (see e.g. Refs. [24,25]).

The almost transparent beam splitters are placed with a density appropriate to the loss rate of the fiber. At the other input ports of each of these impinges the "environment", which at optical frequencies can be approximated as the vacuum state. The resulting state is obtained by omitting the output in the environment modes (i.e. tracing out in these degrees of freedom).

The series of beam splitters can in this case be replaced by a single one, whose transmittance η then depends on the fiber length L. Note that there are cases, e.g. when modeling phase-sensitive reservoirs, when this is not possible [26]. Such a beam splitter, of transmittance η models a lossy fiber with loss rate γ_L and length L such that $\eta = e^{-\gamma_L L}$. Introducing $\gamma = c\gamma_L$ decoherence can be translated to time dependence $\eta(t) = e^{-\gamma t}$.

It can be easily verified that the above model of loss is equivalent to solving the master equation

$$\frac{\mathrm{d}\hat{\varrho}}{\mathrm{d}t} = \frac{\gamma}{2}\left(2\hat{a}\hat{\varrho}\hat{a}^\dagger - \hat{a}^\dagger\hat{a}\hat{\varrho} - \hat{\varrho}\hat{a}^\dagger\hat{a}\right) \tag{15}$$

describing the time evolution in the interaction picture of a damped harmonic oscillator at zero temperature [27]. Here $\hat{a}$ and $\hat{a}^\dagger$ are the annihilation and creation operators of the oscillator, which in our case is a mode of the optical field.

Starting from a mixture of coherent-state superpositions of the form (4), a straightforward calculation shows, that the state emerging from the lossy fiber reads

$$\begin{aligned}\hat{\varrho}(t) = {} & \varrho_{00}\,|\alpha_1'(t)\rangle\langle\alpha_1'(t)| + c(t)^*\varrho_{01}\,|\alpha_1'(t)\rangle\langle\alpha_2'(t)| \\ & + c(t)\varrho_{10}\,|\alpha_2'(t)\rangle\langle\alpha_1'(t)| + \varrho_{11}\,|\alpha_2'(t)\rangle\langle\alpha_2'(t)|\,.\end{aligned} \tag{16}$$

Here we have introduced the the damped coherent amplitudes $\alpha_i'(t) = \sqrt{\eta(t)}\alpha_i$, and

$$c(t) = \left\langle \sqrt{1-\eta(t)}\alpha_1 | \sqrt{1-\eta(t)}\alpha_2 \right\rangle = a^{1-\eta(t)} e^{-2i\chi(1-\eta(t))} \tag{17}$$

is the overlap between the environment's share of the two coherent states. Equation (16) follows from the mere fact that coherent states interfere on the beam splitter as classical amplitudes. Alternatively it may be derived directly from the solution of the master equation of the process given in reference [27]. Note that the decohered state is of the form (4) too, albeit with new coherent amplitudes $\alpha_i'(t)$. As seen above, decoherence is readily described in the nonorthogonal coherent-state basis where the basis vectors "follow" adaptively the time evolution of the state. In what follows, we denote this evolution by operator $\mathcal{D}$: $\varrho(t) = \mathcal{D}(\varrho)$. This evolution formally resembles a phase damping channel [28,29], but one should keep in mind, that the basis is nonorthogonal. In the special case if $\varrho_{00} = \varrho_{11} = 1, \varrho_{01} = \varrho_{10} = -1$, we regain the results for the decoherence of a displaced odd coherent state considered in [10].

Decoherence has a simple form in the nonorthogonal "comoving" coherent-state basis where the basis vectors are $|\alpha_i'(t)\rangle$. However, this basis becomes less and less orthogonal with time. It is of some interest to examine how the parameters describing the state in a suitable *orthogonal* basis change with time. Describing decoherence on a "comoving" qubit basis $|\pm\rangle$ can be done in three steps: (1) revert to the coherent state basis, (2) let decoherence $\mathcal{D}$

act, (3) revert to a new qubit basis. This can be put succinctly as follows:

$$\boldsymbol{\sigma} \longrightarrow \mathbf{T}(t)\mathcal{D}(\mathbf{T}^{-1}\boldsymbol{\sigma}\mathbf{T}^{-1\dagger})\mathbf{T}^{-1\dagger}(t), \tag{18}$$

where the time argument t indicates that the $\mathbf{T}$ matrix (11) corresponding to the decreased amplitudes $\alpha_i'(t) = \sqrt{\eta(t)}\alpha_i$ is to be used.

Following the procedure outlined in the previous paragraph, we have derived the explicit results from (16) for the pseudospin components P_1, P_2 and P_3 of an arbitrary state. We obtain the following path on an adaptive Bloch sphere:

$$P_1(t) = \sqrt{\frac{1-a'(t)^2}{1-a^2}}P_1(0), \tag{19}$$

$$P_2(t) = \frac{a}{a'(t)}\sqrt{\frac{1-a'(t)^2}{1-a^2}}P_2(0), \tag{20}$$

$$P_3(t) = a'(t)\frac{1-(a/a'(t))^2}{1-a^2} + \frac{a}{a'(t)}\frac{1-a'(t)^2}{1-a^2}P_3(0). \tag{21}$$

The time dependence appears through the running overlap $a'(t)$, defined as in equation (3):

$$a'(t) = a^{\eta(t)} = \exp(-2\left|\alpha\right|^2 e^{-\gamma t}). \tag{22}$$

In equations (19–21), $P_k(0)$ denotes the original, and $P_k(t)$ the decohered values.

The effect of decoherence appears in two distinct ways. On one hand, equations (19–21) allow us to follow the time evolution on the Bloch sphere of the state due to decoherence. On the other hand, decoherence does not only change the position of the point respective to the Bloch sphere, but also the meaning of the sphere itself by decreasing the coherent amplitudes. The qubit description should be interpreted in this "comoving" frame. While the movement on the Bloch sphere is a "rather quantum mechanical" feature of the qubits, the modification of the notion of the sphere describes the "classical loss", that is, the decay of a coherent state, which simply loses its amplitude. This description resembles to some extent the interaction picture of quantum mechanics, where both the reference frame of the Hilbert space and the state vector move, due to conceptionally different reasons.

The presented exact results allow us to quickly arrive at the usual solutions in two limiting cases. If $|\alpha| \gg 1$, the constituent coherent states are nearly orthogonal, and the state is a real Schrödinger's cat. If we let $\alpha \to 0$, the state obtained becomes a mixture of superpositions of displaced Fock states $\hat{D}(\beta)\left|0\right\rangle$ and $\hat{D}(\beta)\left|1\right\rangle$ (the differences in decoherence dynamics in these two limiting cases, in connection with squeezing, photon-number distributions and Wigner functions have been analyzed in reference [18]).

In the highly nonclassical large amplitude case $a/a'(t)$ decays fast and exponentially. This can be seen by expanding the factor $e^{-\gamma t}$ in (22) to first order in t, valid for $t \ll 1/\gamma$. The overlap $a'(t)$ then becomes: $a'(t) \approx a\exp(2\left|\alpha\right|^2\gamma t)$, causing $a/a'(t)$ to decay with the familiar characteristic time

$$t_{\mathrm{dec}} = \frac{1}{2\gamma\left|\alpha\right|^2}. \tag{23}$$

For large α, evidently $t_{\mathrm{dec}} \ll 1/\gamma$, and so the above approximation is self-consistent, giving the decay time to a good approximation. As seen from (19–21), the exponential decay leads to the fast reduction of P_2 and P_3 to 0. On the Bloch sphere, the point representing the system falls onto the P_1 axis, which coincides with the classicality line in the large amplitude limit. This is a typical feature of the phase damping channel: the superposition becomes a statistical mixture, conserving the probability weights. The time scale of this process is inversely proportional to the "distance" of the coherent states, as often seen in decoherence processes. On a larger time scale, $a'(t)$ itself increases due to the decay of the coherent amplitude, and this induces the decrease of $\sqrt{(1-a'(t)^2)/(1-a^2)}$ from 1 to 0. The characteristic time for this non-exponential damping process can be found from (19–21),

$$t_{\mathrm{damp}} = \frac{\log\left|\alpha\right|^2}{\gamma}. \tag{24}$$

In the small amplitude, $\alpha < 0.1$ case we find to a good approximation:

$$P_1(t) \approx \sqrt{\eta(t)}P_1(0), \tag{25}$$

$$P_2(t) \approx \sqrt{\eta(t)}P_2(0), \tag{26}$$

$$P_3(t) \approx 1 - \eta(t) + \eta(t)P_3(0). \tag{27}$$

In these we recognize the formulae describing the spontaneous decay of a two-level system. With $\beta = 0$, in the small amplitude case the basis states become the Fock states $\left|0\right\rangle$ and $\left|1\right\rangle$. The physical picture of decoherence is then that the single photon the mode contains leaks at an exponential rate from the optical fiber. A nonzero β means a displacement initially applied to the state, which has no influence on the density matrix in the orthogonal basis. In this case there is a single characteristic time,

$$t_1 = 1/\gamma. \tag{28}$$

The characteristic time is independent of α in the small α limit.

4 Creation of entangled coherent states on a beam splitter, and their decoherence

4.1 Quantification of entanglement

For a pure quantum state $\left|\Psi\right\rangle_{12}$ of two modes the usual measure of quantum correlations is the entropy of entanglement. This is the von Neumann entropy of the reduced density operator of either one of the subsystems,

$$E(\left|\Psi\right\rangle_{12}) = -\mathrm{Tr}_1\left[(\mathrm{Tr}_2\left|\Psi\right\rangle_{12\ 12}\langle\Psi|)\log(\mathrm{Tr}_2\left|\Psi\right\rangle_{12\ 12}\langle\Psi|)\right]. \tag{29}$$

For a pure state of two qubits, this can be written as:

$$E(|\Psi\rangle_{12}) = H\left(\frac{1+\sqrt{1-C^2}}{2}\right). \quad (30)$$

Here $H(x) = -x\log(x) - (1-x)\log(1-x)$ is the binary entropy function, and $C = 2\sqrt{\mathrm{Det}\ (\mathrm{Tr}_1 |\Psi\rangle_{12\ 12}\langle\Psi|)}$, the so-called concurrence, is related to the determinant of the reduced density operator. Both the concurrence C and its square C^2 are useful entanglement measures themselves, reasonably approximating the entropy of entanglement.

For mixed states, the question of entanglement is more Byzantine. The entanglement of formation [30] is defined as the least expected entanglement of any ensemble of pure states realizing the mixed state in question. This is not equal to the distillable entanglement [30], the asymptotic number of pure singlets that can be prepared locally from the mixed state by entanglement purification protocols [31,32]. Although these have straightforward physical interpretation, they are in general not possible to calculate.

The mixed states investigated in this article, however, are interpreted as states of two qubits. Thus, as remarked in [20], their entanglement of formation can be evaluated with the method of Wootters [33]. Wootters has shown that for a mixed state of two qubits, the entanglement of formation is still given by the formula at the right-hand side of (30), albeit the concurrence C now has a different interpretation. It can be expressed in terms of the eigenvalues λ_k (in decreasing order) of the non-Hermitian operator $\hat{\varrho}\tilde{\hat{\varrho}}$, where the tilde denotes the "spin flip" operation:

$$C(\varrho) = \max\{0, \lambda_1 - \lambda_2 - \lambda_3 - \lambda_4\}. \quad (31)$$

The Wootters formula is exact, and can be efficiently evaluated numerically.

4.2 The beam splitter as an entangling device

Consider a beam splitter described by real transmission and reflection coefficients, whose the transmittance is denoted by ξ. As already exploited, coherent states interfere as classical amplitudes, thus if at the input ports there are coherent states, two coherent states appear at the output ports:

$$|\mu\rangle_1 |\lambda\rangle_2 \to |\sqrt{\xi}\mu + \sqrt{1-\xi}\lambda\rangle_3 |\sqrt{1-\xi}\mu - \sqrt{\xi}\lambda\rangle_4. \quad (32)$$

Here indices 1 and 2 refer to the input modes, while 3 and 4 to the output modes, respectively. The output two-mode state is manifestly separable, a sign of the classicality of the coherent state [21]. If, however, one of the input fields is a coherent-state *superposition*, while the other input field is in the vacuum state, it follows directly from the linearity of the beam splitter transformation that the state emerging from the beam splitter,

$$(c_1 |\alpha_1\rangle_1 + c_2 |\alpha_2\rangle_1) |0\rangle_2 \to$$
$$c_1 |\sqrt{\xi}\alpha_1\rangle_3 |\sqrt{1-\xi}\alpha_1\rangle_4 + c_2 |\sqrt{\xi}\alpha_2\rangle_3 |\sqrt{1-\xi}\alpha_2\rangle_4, \quad (33)$$

is not separable. In the following, we will examine this "recipe" for producing entanglement on a beam splitter. Since the vacuum $|0\rangle_2$ has a rotationally invariant Wigner function, our choice of a beam splitter with real parameters does not decrease generality.

Before going into the details, we mention the fact that Weyl displacement of input modes of a beam splitter results in displacement of the output modes. The displacement constants for the output modes are given as the beam splitter transforms of the input displacements. Now since the displacements at the output ports are local unitary operations, they do not affect the amount of entanglement in the two-mode output state. This means that the entanglement between the output modes cannot be changed by displacing the input modes. This simplifies the calculations: we can displace the input state (1) by $-\beta$, and then compute the entanglement it generates.

The amount of entanglement between the two output modes of the beam splitter is readily computable, noticing that each of the modes 3 and 4 examined alone is in a mixed state of the form in equation (4). The output modes can then be treated as qubits, meaning that a two-qubit state leaves the beam splitter. The entanglement between the modes is therefore never more than 1 ebit, and depends on the probability amplitudes c_1, c_2, the coherent amplitude α, and the transmittance ξ. As is expected intuitively, the amount of entanglement is highest for a symmetric beam splitter ($\xi = 1/2$). A surprising fact is that $|-\rangle$ leads to 1 ebit of entanglement irrespective of α and β, as noted in reference [10].

We therefore set $\xi = 1/2$, and pose the question, how much entanglement we can generate from a mixed coherent-state qubit as in equation (4) (given $\boldsymbol{\sigma}$) by "halving" it on a beam splitter. Although we are dealing with pure states at this stage, we have performed calculations for general mixtures in the Bloch sphere picture. The density matrix of the two-mode state in the qubit basis reads:

$$\boldsymbol{\sigma}^{(34)} = \frac{1}{2}\begin{pmatrix} \sigma_{00}\frac{(1+\sqrt{a})^2}{1+a} & \sigma_{01}\frac{1+\sqrt{a}}{\sqrt{1+a}} & \sigma_{01}\frac{1+\sqrt{a}}{\sqrt{1+a}} & \sigma_{00}\frac{1-a}{1+a} \\ \sigma_{10}\frac{1+\sqrt{a}}{\sqrt{1+a}} & \sigma_{11} & \sigma_{11} & \sigma_{10}\frac{1-\sqrt{a}}{\sqrt{1+a}} \\ \sigma_{10}\frac{1+\sqrt{a}}{\sqrt{1+a}} & \sigma_{11} & \sigma_{11} & \sigma_{10}\frac{1-\sqrt{a}}{\sqrt{1+a}} \\ \sigma_{00}\frac{1-a}{1+a} & \sigma_{01}\frac{1-\sqrt{a}}{\sqrt{1+a}} & \sigma_{01}\frac{1-\sqrt{a}}{\sqrt{1+a}} & \sigma_{00}\frac{(1-\sqrt{a})^2}{1+a} \end{pmatrix}. \quad (34)$$

If the input state is pure, so is the output, and its entanglement can be quantified by the entropy of entanglement. To evaluate this we need to trace over mode 4 in (34) to obtain the reduced density matrix of mode 3,

$$\boldsymbol{\sigma}^{(3)} = \frac{1}{2}\begin{pmatrix} 1+\frac{\sqrt{a}}{1+a}(1+P_3) & \frac{1}{\sqrt{1+a}}(P_1 - i\sqrt{a}P_2) \\ \frac{1}{\sqrt{1+a}}(P_1 + i\sqrt{a}P_2) & 1-\frac{\sqrt{a}}{1+a}(1-P_3) \end{pmatrix}, \quad (35)$$

where P_i are the pseudospin components of the original one-mode state $\boldsymbol{\sigma}$. The square of the concurrence can be evaluated from $\boldsymbol{\sigma}^{(3)}$ as a function of the pseudospin

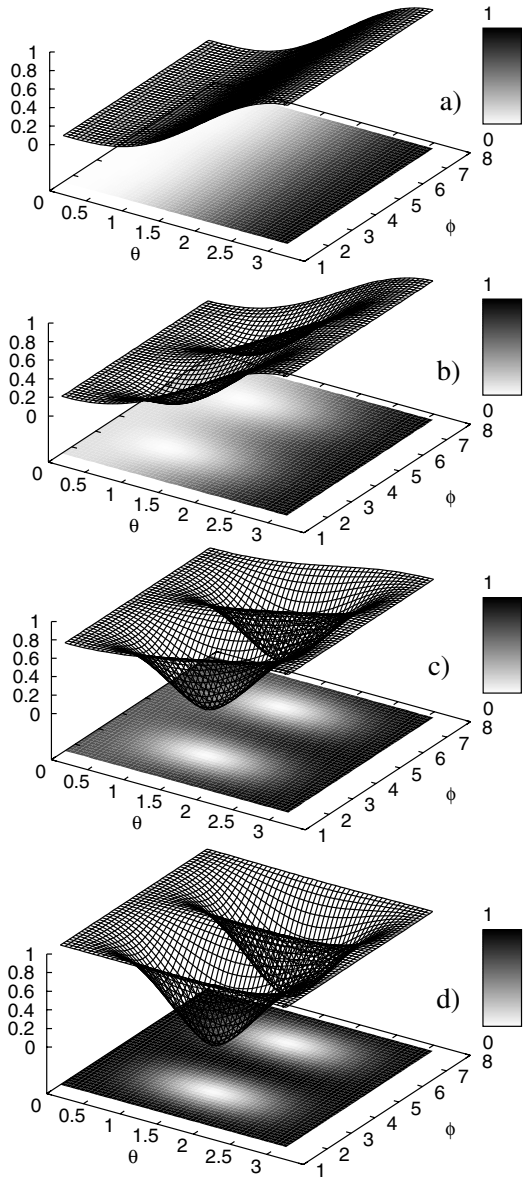

Fig. 2. The entanglement of states obtained by splitting a coherent-state qubit on a 50:50 real beam splitter. The entropy of entanglement is plotted against the angles θ and ϕ specifying the superposition, for (a) $\alpha = 0.1$, (b) $\alpha = 0.5$, (c) $\alpha = 1$, and (d) $\alpha = 2.5$.

components of the input state:

$$C^2 = \frac{1}{(1+a)^2}\left(1 + a^2 - (P_1)^2 - a^2(P_2)^2 - 2aP_3\right). \quad (36)$$

From this, according to equation (30) we obtain the entanglement that can be produced from a pure coherent-state superposition with given pseudospin components. In Figure 2 this is plotted for four different values of α as a function of the initial parameters θ and ϕ defined in equation (14).

In the "highly nonclassical" regime, $a \ll 1$, and therefore $C^2 \approx 1 - (P_1)^2$. This shows that to have a large amount of entanglement, P_1 should be 0. Since in this regime the P_1 axis coincides with the classicality line, this implies that the state should have an equal weight of $|\alpha\rangle$ and $|-\alpha\rangle$ in it. In this case $|\alpha\rangle$ and $|-\alpha\rangle$ are approximately orthogonal, and so

$$c_1 \left|\alpha/\sqrt{2}\right\rangle_3 \left|\alpha/\sqrt{2}\right\rangle_4 + c_2 \left|-\alpha/\sqrt{2}\right\rangle_3 \left|-\alpha/\sqrt{2}\right\rangle_4$$

is approximately the Schmidt decomposition.

In the small amplitude, $|\alpha| \ll 1$ limit, $a \approx 1$, and therefore we can approximate the square of the concurrence (36) as: $C^2 \approx 1/4(2 - (P_1)^2 - (P_2)^2 - 2P_3)$, which is obviously maximized for $P_3 \approx 1$. This, in the small amplitude case, is just the single-photon Fock state $|1\rangle$, showing, as expected, that for a superposition of $|0\rangle$ and $|1\rangle$ to gain maximum entanglement we have to suppress the vacuum as much as possible.

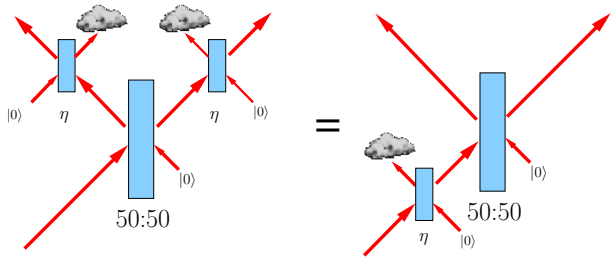

Fig. 3. Symmetric decoherence at the output ports of a 50:50 beam splitter is equivalent to decoherence with the same rate at the input port.

4.3 Decoherence and loss of entanglement in two-mode entangled coherent states

We now turn our attention to the effect of loss on the entanglement. Each of the modes leaving the beam splitter are subjected to decoherence due to loss in a way described in Section 3. In the general case, the loss rates γ_L for the two modes are different. After changing to the proper orthogonal basis in each of the modes, as described in Section 2, we can still treat the two-mode partially decohered state as a two-qubit state. This allows us to use the Wootters formula, and calculate explicitly the entanglement of formation. For the sake of further simplicity we consider the case of symmetric decoherence, i.e. we set the decoherence rates γ_L equal for the two output modes.

If the decoherence rates in modes 3 and 4 are equal, then, as illustrated in Figure 3, creating the two-mode state first and then letting decoherence act, or letting the qubit decohere first and then using the beam splitter, leads to exactly the same state [25]. Our calculations thus have a double interpretation. They can either be read as describing the loss of entanglement in a two-mode entangled coherent state, or as the loss of some nonclassical property of a one-mode coherent-state superposition, making it less useful for creating entanglement.

We have evaluated numerically the entanglement of formation for different initial parameters, as a function

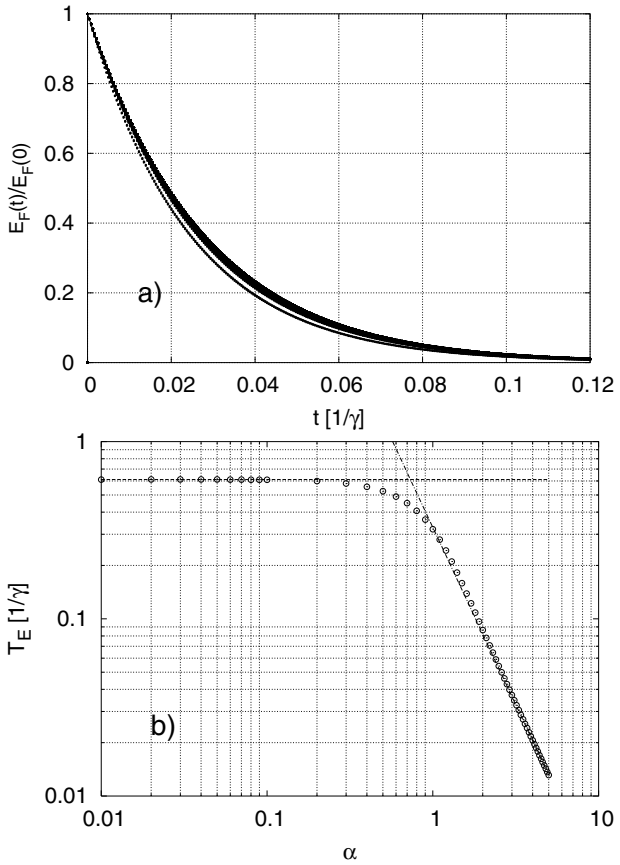

Fig. 4. The loss of entanglement due to decoherence. For entangled two-mode coherent states with the same initial amplitude $\alpha = 3.5$ but different superposition weights c_1 and c_2, in (a) plot the fraction of the original entanglement left after some time t during which the state suffers decoherence. In (b) we show the dependence of the characteristic time T_E of entanglement loss on the coherent amplitude α, in a log-log plot. The slashed line is the constant value $T_E \approx 0.61$ attained for small α, the slashed-dotted line is the function $1/(3\gamma\,|\alpha|^2)$, which describes the behavior of T_E in the large amplitude limit.

of decoherence time. We have found that the entanglement of formation decays exponentially with time. The characteristic time T_E of the loss of entanglement is approximately independent of the initial state's θ and ϕ, especially for large α, as illustrated in Figure 4a. There is a strong dependence of this characteristic time, however, on the coherent amplitude α, shown in Figure 4b. In the asymptotic cases of $\alpha \ll 1$ and $\alpha \gg 1$, the entanglement decay time T_E is proportional to the decoherence times found in Section 3, in equations (28, 23). The constant of proportionality is somewhat different in the small and large α case, being 0.61 for the first and 0.66 for the second.

The following conclusions can be drawn regarding the loss of entanglement due to decoherence. First, the loss of entanglement is independent of the superposition amplitudes c_1 and c_2 of the coherent states. After a certain time t a fixed ratio of the original entanglement is lost, and this ratio depends only on t and the original coherent amplitude α. From this, two conclusions can be drawn. If for a given coherent amplitude α a specific pure superposition is q times better for entanglement production than another one with different probability amplitudes, then this ratio remains valid after any amount of decoherence as well. Secondly, the time scale for the loss of entanglement in the two-mode state is similar to the decoherence time for the original one-mode state from which it was produced, differing by a factor of approximately 2/3.

A few remarks concerning the role of the displacement (Eq. (2)) of a coherent-state superposition are in order. As discussed above, such displacements do not influence the amount of entanglement that is generated from the state on any beam splitter. This is also the reason why they do not influence the decoherence time scale of a coherent-state superposition. For states with $\beta = 0$, i.e., $c_1\,|\alpha\rangle + c_2\,|-\alpha\rangle$, the nonclassicality, and the entanglement generated from the state, are destroyed by decoherence during the same time duration, which is required for one photon to be lost. Roughly on may claim that a lost photon (or, as it be, the fact that no photon was lost) contains essentially all information about the state. This is of course not true after displacement by β: the decoherence time remains the same, but the number of photons lost during that time can be substantially higher or lower. States with very high β are superpositions of semiclassical states whose nonclassicality survives the loss of many photons.

5 Conclusions

The superposition of any two coherent states can be used to represent a qubit. The qubit's value (i.e., its state) is distorted due to decoherence processes. We have provided a full description of the effect of a lossy transmission line on a superposition of arbitrary two coherent states. We have introduced the adaptive Bloch sphere to discuss the quantum effects of the so arising decoherence, and have derived the exact expressions describing the trajectory of the system.

An advantage of the coherent-state qubit is that entanglement is easily created on a beam splitter. We have calculated the amount of entanglement that can be produced from an arbitrary qubit state by splitting it on a beam splitter, and have investigated the effect of decoherence on the resulting entangled state. We have found that entanglement is lost on the time scale of decoherence of the initial qubit. Moreover, entanglement is lost uniformly: given the overlap between the constituent coherent states, the percentage of the entanglement (of formation) remaining in the state after some decoherence is independent of the phases and the moduli of the probability amplitudes.

This work was supported by the National Scientific Research Fund of Hungary (OTKA) under contracts Nos. T034484, T043079, and T043287. M.K. acknowledges the support of the European Union Network "CONQUEST".

References

1. E. Schrödinger, Naturwissenschaften **23**, 807 (1935)
2. V.V. Dodonov, I.A. Malkin, V.I. Man'ko, Physica **72**, 597 (1973)
3. M. Brune et al., Phys. Rev. Lett. **77**, 4887 (1996)
4. C. Monroe, D.M. Meekhof, B.E. King, D.J. Wineland, Science **272**, 1131 (1996)
5. B. Yurke, D. Stoler, Phys. Rev. Lett. **57**, 13 (1986)
6. M.G.A. Paris, J. Opt. B-Quant. Semicl. Opt. **1**, 662 (1999)
7. B.C. Sanders, Phys. Rev. A **45**, 6811 (1992)
8. M. Paternostro, M.S. Kim, B.S. Ham, Phys. Rev. A **67**, 023811 (2003)
9. J. Janszky, A.V. Vinogradov, Phys. Rev. Lett. **64**, 2771 (1990)
10. S.J. van Enk, O. Hirota, Phys. Rev. A **64**, 022313 (2001)
11. H. Jeong, M.S. Kim, J. Lee, Phys. Rev. A **64**, 052308 (2001)
12. H. Jeong, M.S. Kim, Phys. Rev. A **65**, 042305 (2002)
13. T.C. Ralph et al., Phys. Rev. A **68**, 042319 (2003)
14. J. Janszky et al., Quant. Semiclass. Opt. **7**, 145 (1995)
15. R. Filip, J. Perina, J. Opt. B-Quant. Semicl. Opt. **3**, 21 (2001)
16. F.A.A. El-Orany, J. Perina, V. Perinova, M.S. Abdalla, J. Opt. B-Quant. Semicl. Opt. **4**, S153 (2002)
17. F.A.A. El-Orany, J. Perina, V. Perinova, M.S. Abdalla, Eur. Phys. J. D **22**, 141 (2003)
18. J. Calsamiglia, S.M. Barnett, N. Lütkenhaus, K.-A. Suominnen, Phys. Rev. A **65**, 043814 (2001)
19. P. Foldi, M.G. Benedict, A. Czirjak, B. Molnar, Phys. Rev. A **67**, 032104 (2003)
20. S.-B. Li, J.-B. Xu, Phys. Lett. A **309**, 321 (2003)
21. Y. Aharonov, D. Falkoff, E. Lerner, H. Pendleton, Ann. Phys. **39**, 498 (1966)
22. M.S. Kim, W. Son, V. Bužek, P.L. Knight, Phys. Rev. A **65**, 032323 (2002)
23. J. Janszky et al., Fortschr. Phys. **51**, 157 (2003)
24. R.A. Campos, B.E.A. Saleh, M.C. Teich, Phys. Rev. A **40**, 1371 (1989)
25. U. Leonhardt, *Measuring the Quantum State of Light* (Cambridge University Press, The Edinburgh Building, Cambridge, CB2 2RU, UK, 1997)
26. M.S. Kim, N. Imoto, Phys. Rev. A **52**, 2401 (1995)
27. S.J.D. Phoenix, Phys. Rev. A **41**, 5132 (1990)
28. M.A. Nielsen, I.L. Chuang, *Quantum Computation and Quantum Information* (Cambridge University Press, The Edinburgh Building, Cambridge, CB2 2RU, UK, 2000)
29. J. Preskill, Lecture Notes for Physics 229: Quantum information and computation, available at `http://www.theory.caltech.edu/people/preskill` (1998)
30. C.H. Bennett, D.P. DiVincenzo, J.A. Smolin, W.K. Wootters, Phys. Rev. A **54**, 3824 (1996)
31. H. Jeong, M.S. Kim, Quant. Inf. Comp. **2**, 208 (2002)
32. J. Clausen, L. Knöll, D.-G. Welsch, Phys. Rev. A **66**, 062303 (2002)
33. W.K. Wootters, Phys. Rev. Lett. **80**, 2245 (1998)